Electronic Supplementary Material (ESI) for Nanoscale.

Supplementary Information

Synthetic DNA nanopores for direct molecular transmission between lipid vesicles

Zugui Peng,[‡a] Shoichiro Kanno,[‡a] Kenta Shimba,[b] Yoshitaka Miyamoto,[ac] Tohru Yagi[*a]

[a.] School of Engineering, Tokyo Institute of Technology, 403, Ishikawadai Bldg. 3, 2-12-1 Ookayama, Meguro-ku, Tokyo 152-8550 Japan
E-mail: yagi.t.ab@m.titech.ac.jp

[b.] Graduate School of Frontier Sciences, The University of Tokyo, 5-1-5, Kashiwanoha, Kashiwa, Chiba 277-8563, Japan

[c.] Department of Maternal-Fetal Biology, National Research Institute for Child Health and Development, 2-10-1 Okura, Setagaya-ku, Tokyo 157-8535, Japan

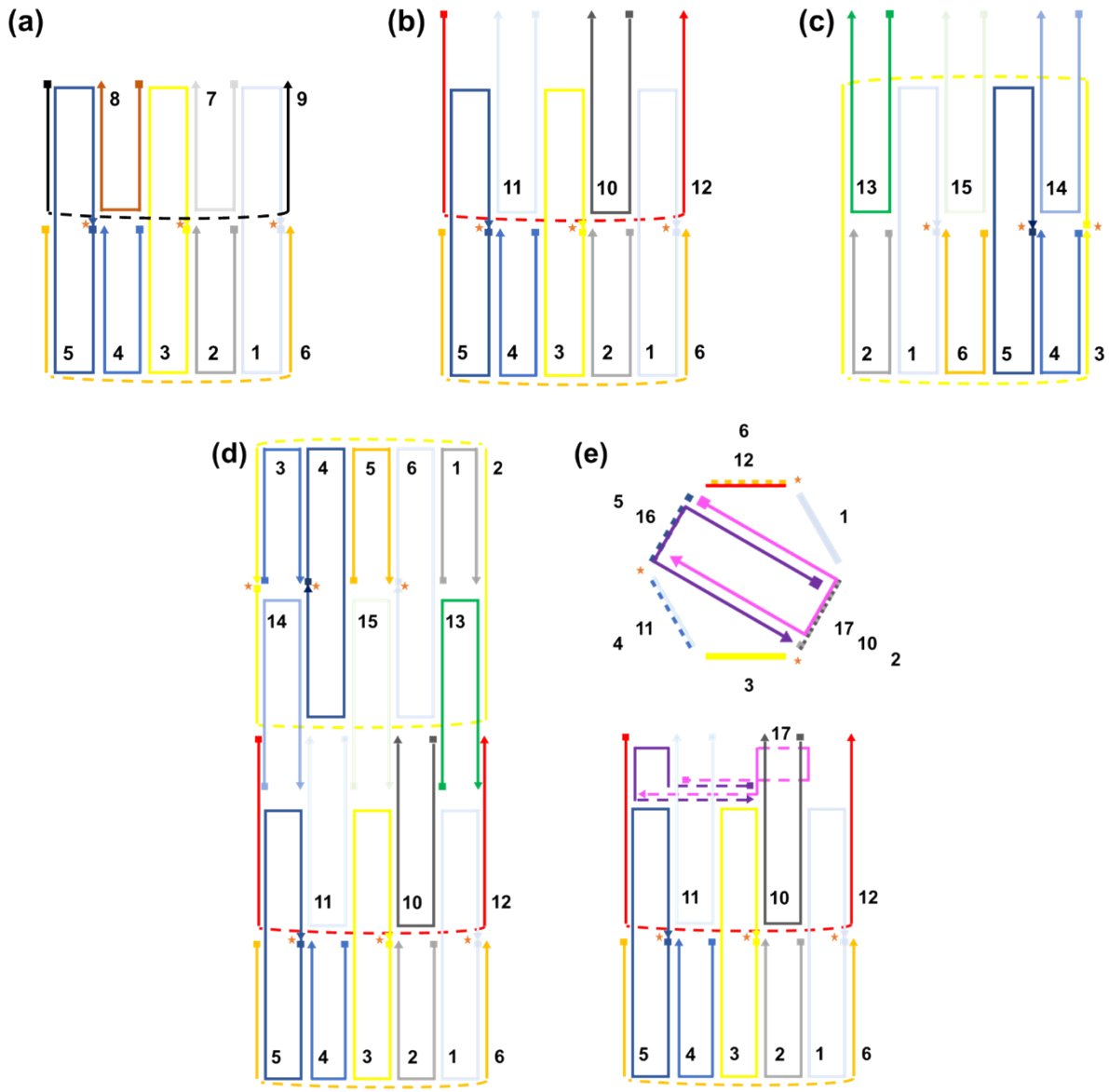

Fig S1. Two-dimensional map of DNA nanopores (a) $\mathbf{A^C_{short}}$, (b) $\mathbf{A^C}$, (c) $\mathbf{B^C}$, (d) $\mathbf{(AB)^C}$, and (e) $\mathbf{A^C_{lock}}$. The component DNA strands are represented as lines. Squares and triangles represent the 5′ and 3′ termini of the strands, and the orange stars in the two-dimensional maps indicate cholesterol tags.

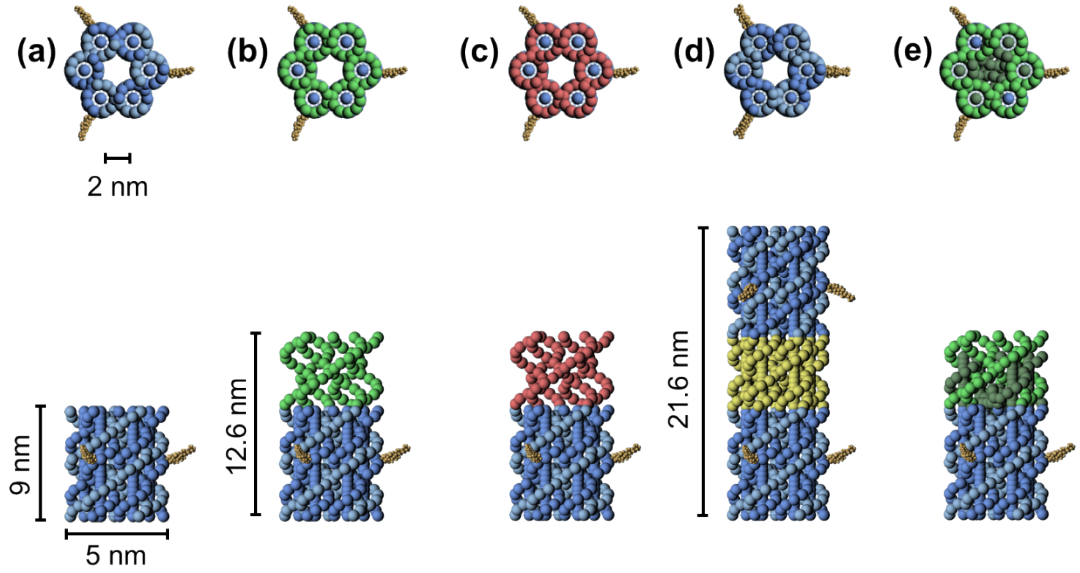

Fig S2. Side and top views of (a) $\mathbf{A^C_{short}}$, (b) $\mathbf{A^C}$, (c) $\mathbf{B^C}$, (d) $\mathbf{(AB)^C}$, and (e) $\mathbf{A^C_{lock}}$ and their dimensions. The double helixes in DNA nanopores are shown in blue and the cholesterol tags are shown in orange. The sticky-end segments of $\mathbf{A^C}$ and $\mathbf{B^C}$ are shown in green and red, whereas the double helix structure formed by the binding of $\mathbf{A^C}$ and $\mathbf{B^C}$ is shown in yellow. Two 40-nucleotide single-strands (**lock**) bound to sticky-end-**A** of $\mathbf{A^C_{lock}}$ are shown in dark green.

Table S1. ID, sequences and chemical modification of the DNA strands used for constructing the DNA nanopores.

ID	Sequences (5' → 3')
1	AGCGAACGTGGATTTTGTCCGACATCGGCAAGCTCCCTTTTTCGACTATT
2	CCGATGTCGGACTTTTACACGATCTTCG
3	CGAAGATCGTGTTTTTCCACAGTTGATTGCCCTTCACTTTTCCCAGCAGG
4	AATCAACTGTGGTTTTTCTCACTGGTGA
5	TCACCAGTGAGATTTTTGTCGTACCAGGTGCATGGATTTTTGCATTCTAA
6	CCTGGTACGACATTTTTCCACGTTCGCT
7	GGGAGCTTGACTGCTGGG
8	GTGAAGGGCTTAGAATGC
9	ATCCATGCAAATAGTCGA
10	TCACCAGTGAGACGGGGAGCTTGACTGCTGGGGCCTATCGTCCGAT
11	CGAGCTAGCATGAAGTGAAGGGCTTAGAATGCACTGCTAGCCTTCA
12	AAGGTCAATGCAAGATCCATGCAAATAGTCGAGCAGTACCGTTCAA
13	CGTCTCACTGGTGAGGGAGCTTGCCTGCTGGGTTGAACGGTACTGC
14	CTTGCATTGACCTTGTGAAGGGCTTAGAATGCTGAAGGCTAGCAGT
15	TTCATGCTAGCTCGATCCATGCAAATAGTCGAATCGGACGATAGGC
16	GTCCGCTTCTTGCATTGATTTTGGCTAGCAGTTTGCGACC
17	GCGGACTTCGTCTCACTGTTTTGACGATAGGCTTGGTCGC
1C	Sequence of 1 carrying a cholesterol via TEG linker at the 3' terminus
3C	Sequence of 3 carrying a cholesterol via TEG linker at the 3' terminus
5C	Sequence of 5 carrying a cholesterol via TEG linker at the 3' terminus
4FAM	Sequence of 4 carrying a FAM at the 3' terminus
4Cy5	Sequence of 4 carrying a Cy5 at the 3' terminus

Table S2. Names and compositions of the DNA nanopores.

Nanopore	ssDNA used
A	**1, 2, 3, 4, 5, 6, 10, 11, 12**
B	**1, 2, 3, 4, 5, 6, 13, 14, 15**
A_{lock}	**1, 2, 3, 4, 5, 6, 10, 11, 12, 16, 17**
A^{C}	**1C, 2, 3C, 4, 5C, 6, 10, 11, 12**
B^{C}	**1C, 2, 3C, 4, 5C, 6, 13, 14, 15**
A^{C}_{short}	**1C, 2, 3C, 4, 5C, 6, 7, 8, 9**
A^{C}_{lock}	**1C, 2, 3C, 4, 5C, 6, 10, 11, 12, 16, 17**
$^{FAM}A^{C}$	**1C, 2, 3C, 4FAM, 5C, 6, 10, 11, 12**
$^{Cy5}B^{C}$	**1C, 2, 3C, 4Cy5, 5C, 6, 13, 14, 15**

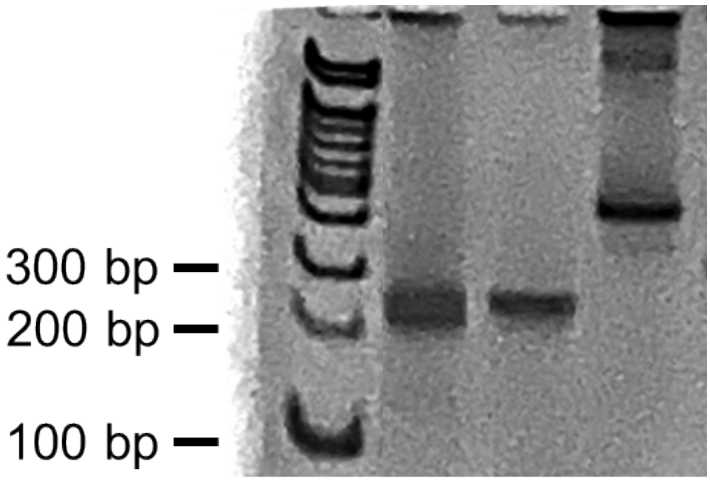

Fig S3. Image of a 5% polyacrylamide gel after electrophoresis, indicating the assembly and binding of DNA nanopores A^C and B^C. Gel lanes from left to right: 100 bp DNA ladder, A^C, B^C, and a mixture of A^C and B^C at 25 °C.

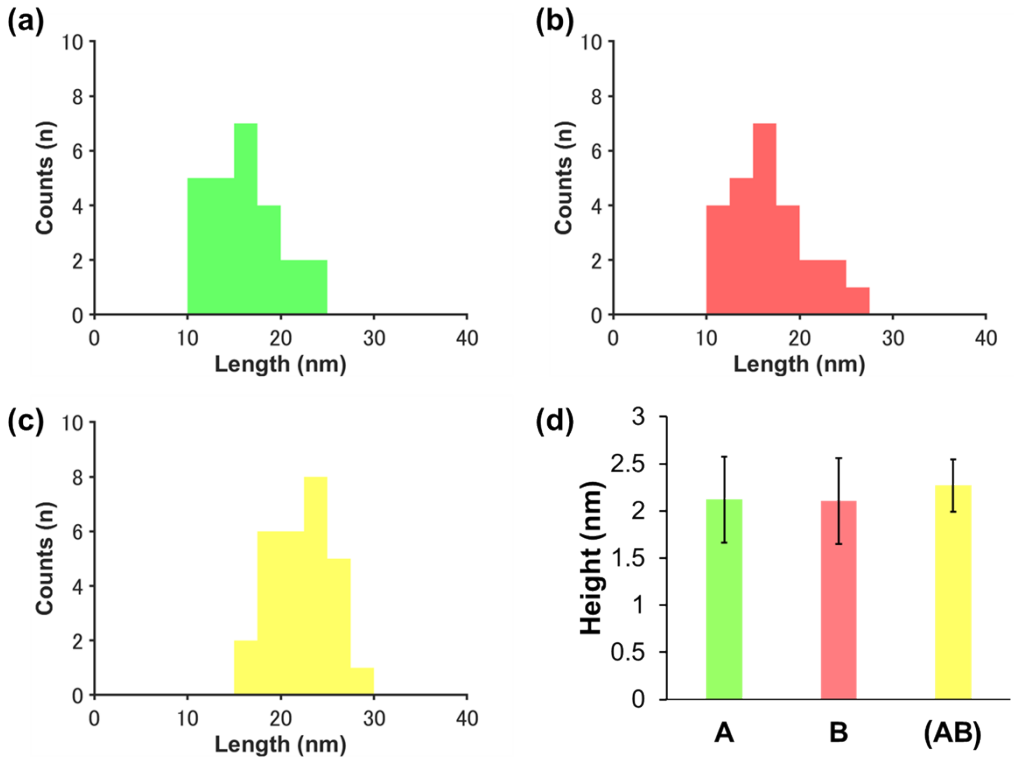

Fig S4. Histograms of the length of (a) **A**, (b) **B**, and (c) **(AB)**. (d) Histogram of the height of **A**, **B**, and **(AB)** acquired from the AFM measurements (*n* = 27, error bars represent SD).

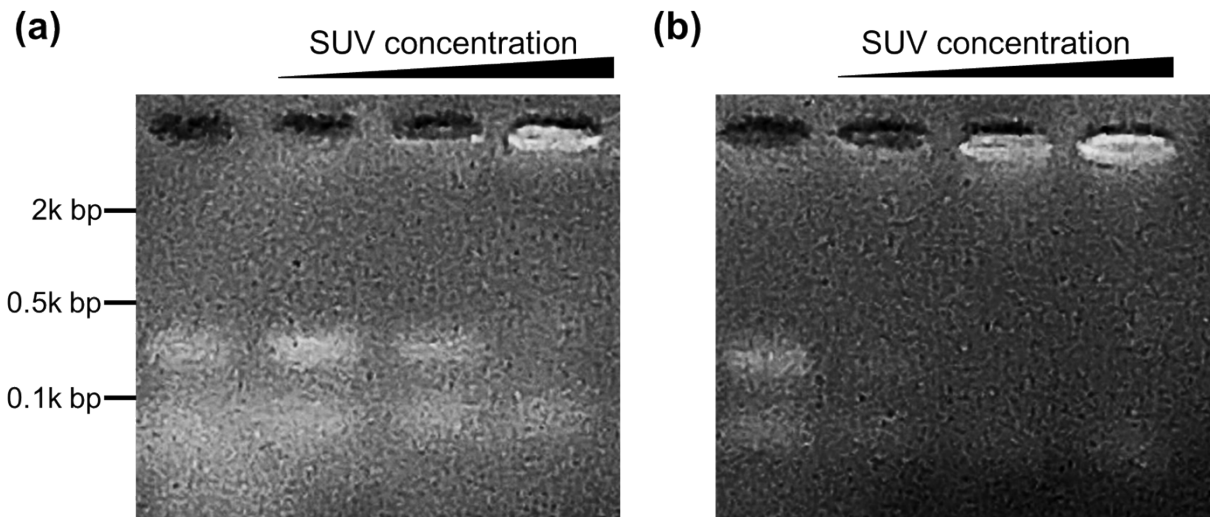

Fig S5. Image of the SUV tethering assay of (a) $\mathbf{A}^{C}$ and (b) $\mathbf{B}^{C}$. Increasing the concentration of SUVs led to more DNA nanopores tethering to SUVs. The position and base pair length of the DNA ladders are shown to the left of the gels.

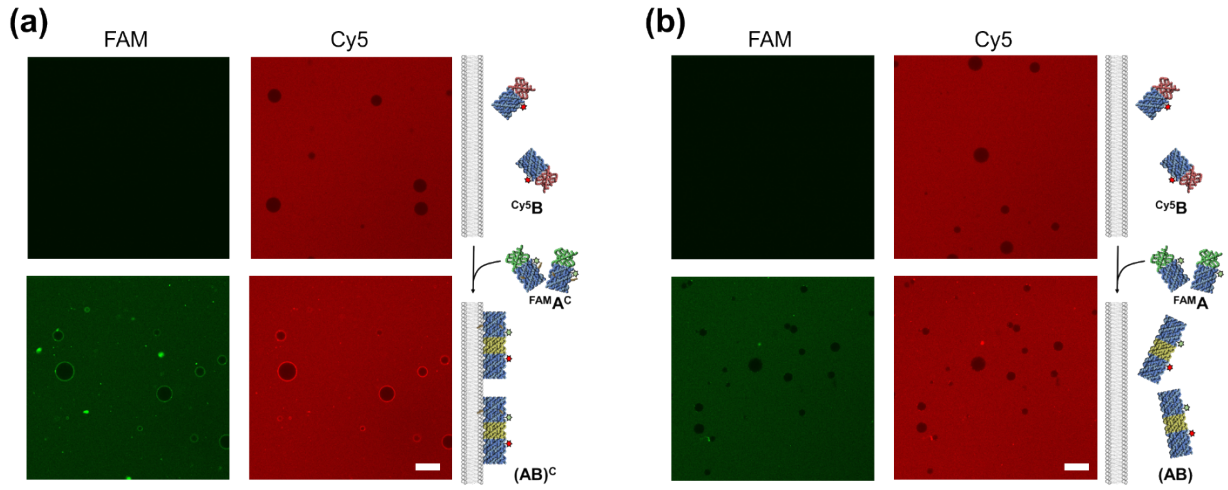

Fig S6. (a) GUVs incubated with $^{Cy5}\mathbf{B}$ observed in fluorescence mode before and after the addition of $^{FAM}\mathbf{A}^{C}$. (b) GUVs incubated with $^{Cy5}\mathbf{B}$ observed before and after the addition of $^{FAM}\mathbf{A}$. Scale bars, 50 µm.

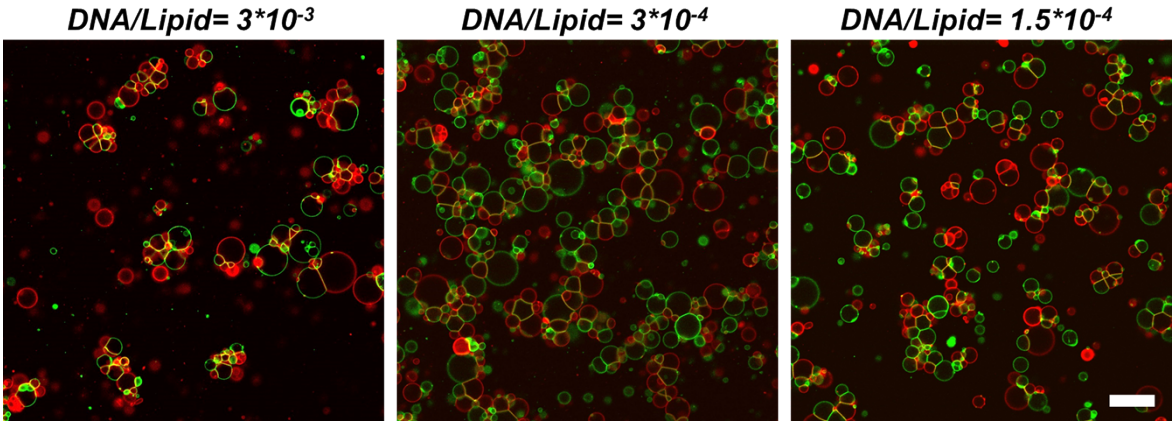

Fig S7. Connection of GUVs using different concentrations of DNA per lipid. DNA nanopores $\mathbf{A^C}$ and $\mathbf{B^C}$ were used. Scale bar, 50 µm.

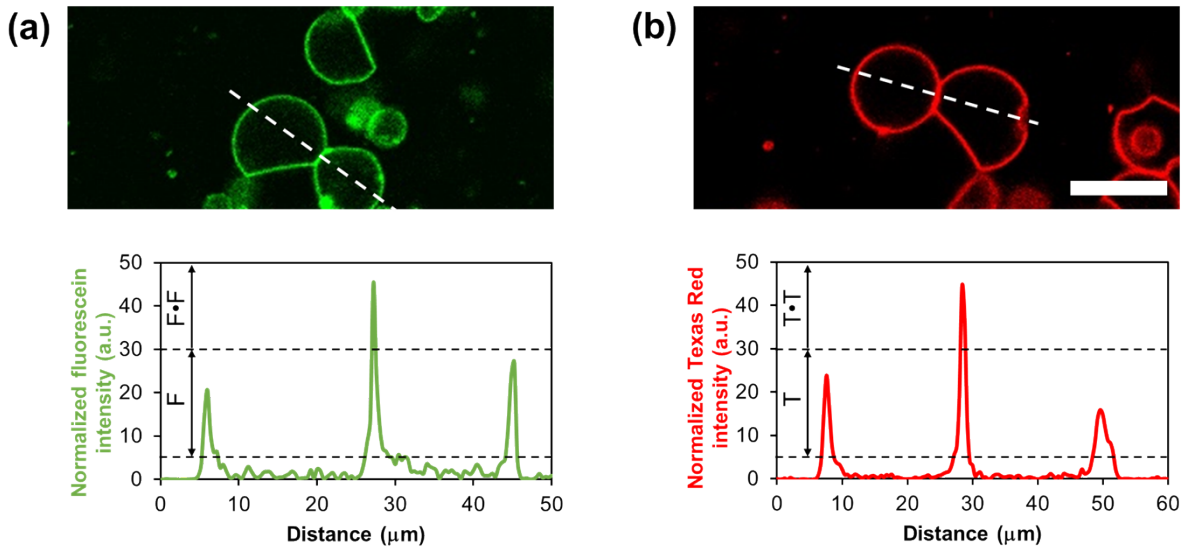

Fig S8. CLSM image and the corresponding fluorescence intensity profiles of (a) connected F-GUVs and (b) T-GUVs functionalized with $\mathbf{A^C}$ and $\mathbf{B^C}$. Scale bar, 25 µm.

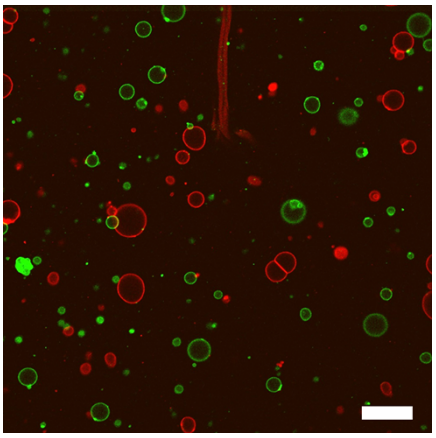

Fig S9. Image of fluorescein-labeled and Texas Red-labeled GUVs without DNA nanopores. Scale bar, 50 µm.

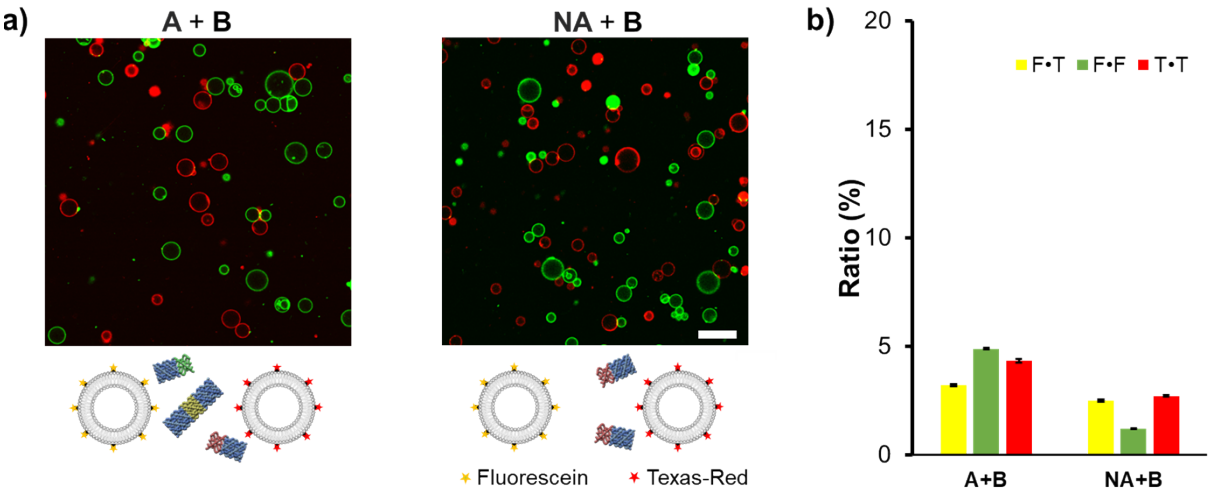

Fig S10. (a) Interactions between fluorescein-labeled and Texas Red-labeled GUVs functionalized with i) **A** and **B**, and ii) only **B**. Ratio of pixels containing signals from both fluorescein and Texas Red, signals from overlapped fluorescein, and signals from overlapped Texas Red (defined as "F·T," "F·F," and "T·T" respectively) among all pixels from images of GUVs incubated with i) **A** and **B**, and ii) only **B**. Scale bar, 50 µm.

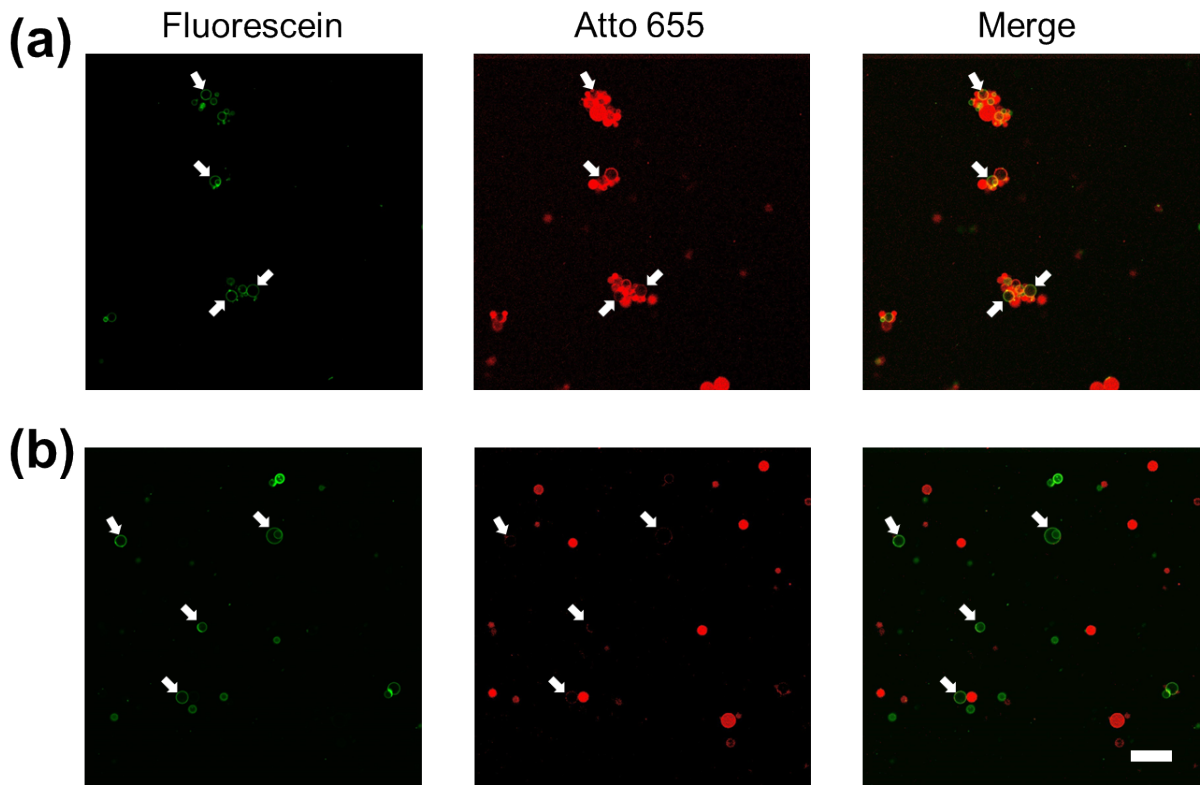

Fig S11. Extra overview images of (a) connected and (b) unconnected GUVs. GUVs labeled with fluorescein (green) and encapsulated with Atto 655 (red) but without membrane labeling were used. The white arrows indicate fluorescein-labeled GUVs. Scale bar, 50 µm.

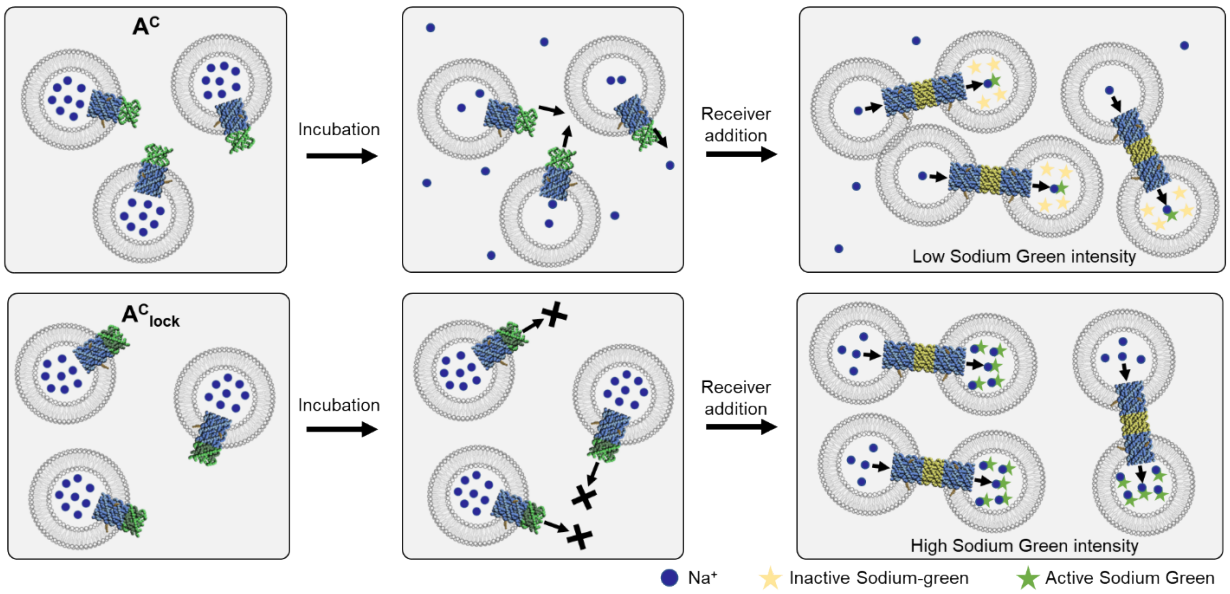

Fig S12. Schematic of Sodium Green assay using SUVs incorporating $\mathbf{A^C}$ and $\mathbf{A^C_{lock}}$. $\mathbf{A^C}$ and $\mathbf{A^C_{lock}}$ were pre-incubated with sender SUVs encapsulating NaCl in a nanopore-to-SUVs ratio of approximately 1:1 for 30 min before use, and B^C was pre-incubated with receiver SUVs encapsulating Sodium Green. During the incubation, Na^+ would leak out only through $\mathbf{A^C}$, and hence the Na^+ concentration in SUVs incorporating $\mathbf{A^C_{lock}}$ would be higher than SUVs incorporating $\mathbf{A^C}$. Due to the higher Na^+ concentration, SUVs incorporating $\mathbf{A^C_{lock}}$ would trigger more Na^+–Sodium Green binding than SUVs incorporating $\mathbf{A^C}$, which would be reflected by a faster increase in Sodium Green fluorescence intensity.

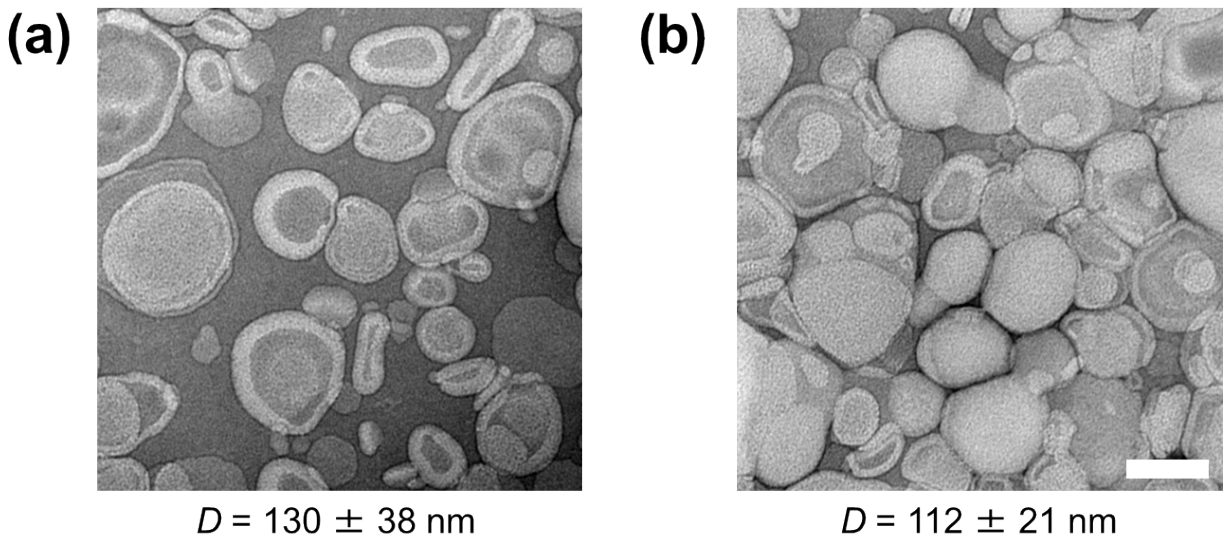

Fig S13. TEM image of (a) SUVs without DNA incorporation and (b) SUVs with incorporated A^C and B^C. Average diameter *D* of 27 SUVs is shown below the images. Scale bar, 100 nm.